Geologische Rundschau 76/3 | 903–922 | Stuttgart 1987

Metallogenesis of cratonic oolitic ironstone deposits in the Bled el Mass, Azzel Matti, Ahnet and Mouydir basins, Central Sahara, Algeria

By Salah Guerrak, Rennes*)

With 12 figures and 8 tables

Zusammenfassung

Die Gebiete des Bled el Mass, des Azzel Matti, des Ahnet und des Mouydir, liegen im Nordwesten des Touaregschildes (Zentral Sahara, Algerian). Neun eisenoolithische Horizonte sind hier in die devonischen Sedimente eingeschaltet. Ihr Mineralinhalt kann durch vier verschiedene Paragenesen charakterisiert werden:

P1 = Chamosit + Magnetit + Maghemit + Goethit; P2 = Chamosit + Hämatit + Goethit + Kalzit; P3 = Chamosit + Hämatit + Goethit + Quartz; P4 = Chamosit + Hämatit + Goethit.

Vier vererzte Fazies Typen treten auf: FOD: (die Ooide sind in einer detritischen Marix eingelagert); FOND: (die Ooide sind in einer nichtdetritischen Matrix eingelagert); FOC: (die Ooide sind verfestigt); FMC: microkonglomeratische Fazies.

Die Ooide entwickeln sich in ruhigen Bedingungen, in Lagunen oder Meerbusen, durch die Bildung von Konkretionen im Sediment aus einem silikatischen und eisenreichen Schlamm; sie werden dann wie detritische Komponenten aufgenommen und transportiert.

Die eisenoolitischen Ablagerungen scheinen durch mehrere Sedimentationsphasen während des Devons entstanden zu sein; so können sie als Zeichen von Sedimentmikrozyklen betrachtet werden. Diese oolitischen Sedimente sind charakteristisch für eine Kratonsedimentation am Rand eines breiten, epikontinentalen Meeres.

Der Usprung des Eisens ist in einem südlichen Kontinent zu suchen, wahrscheinlich in dem mobilen panafrikanischen Gebirge von Nigeria, oder auf dem kongolesischen Schild.

Diese Erze der Zentralsahara können als ein wichtiger Zweig des Eisengürtels betrachtet werden, der sich in Nordafrika von Rio de Oro bis Libyen erstreckt.

Abstract

The Bled el Mass, Azzel Matti, Ahnet and Mouydir areas are located in the northwest of the Touareg Shield (Central Sahara, Algeria). Within the Devonian sedimentary formations, nine oolitic ironstone occurrences of EXID type (Extensive Ironstone Deposition) are interbedded.

Their mineralogical composition is characterized by four different paragenetic associations: P1 (Chamosite – magnetite – maghemite – goethite); P2 (chamosite – hematite – goethite – calcite); P3 (chamosite – hematite– goethite – quartz); and P4 (chamosite – hematite – goethite). Using textural analysis, four main ironstone facies are distinguished: FOD (ooliths scattered in a detrital groundmass); FOND (ooliths scattered in a non detrital groundmass); FOC (cemented ooliths) and FMC (microconglomeratic facies).

Primarily developed in calm conditions by intrasedimentary processes within an iron-rich silicated mud, in lagoons or embayments, ooliths subsequently acquired a detrital character.

The ironstone deposition seems to be induced by several pulses of sedimentation through the Devonian and is considered as indicator of sedimentary subcycles. Therefore, the oolitic ferriferous sediments indicate a cratonic sedimentation on the borders of a large epicontinental sea. The source of the iron could be a remote southern continent, probably the Pan-African mobile belt of Nigeria and the Congo Shield.

The ironstones of the Central Sahara can be considered as an important branch of the North-African Oolitic Ironstone Belt, extending from Rio de Oro to Libya.

Résumé

Les régions du Bled el Mass, de l'Azzel Matti, de l'Ahnet et du Mouydir sont situées au Nord-Ouest du Bouclier Touareg (Sahara Central, Algérie). Neuf niveaux de minerai de fer oolithique sont interstratifiés dans les formations sédimentaires du Dévonien.

Quatre différentes paragenèses caractérisent la composition minéralogique de ces minerais. P1 (chamosite – magnétite – maghémite – goethite); P2 (chamosite – hématite – goethite – calcite); P3 (chamosite – hématite – goethite – quartz) et P4 (chamosite – hématite – goethite).

Quatre facies minéralisés ont été en évidence: FOD (oolithes dispersées dans une matrice détritique); FOND (oolithes dispersées dans une matrice non détritique); FOC (oolithes cimentées) et FMC (faciès microconglomératique).

Développées dans des conditions calmes par concrétionnement intrasédimentaire dans une boue silicatée riche en

*) Author's address: Dr. S. Guerrak, Centre Armoricain d'Etude Structurale des Socles, Laboratoire de Pétrologie Sédimentaire, Institut de Géologie, Université de Rennes I, Avenue du Général Leclerc, 35402 Rennes Cedex, France.

fer, dans des lagons ou des baies, les oolithes vont acquérir par la suite un comportement détritique.

Les dépôts de minerai oolithique semblent avoir été induits par plusieurs pulsations sédimentaires durant le Dévonien et peuvent être ainsi considérés comme des marqueurs de microcycles sédimentaires.

Ces sédiments oolithiques sont caractéristiques d'une sédimentation cratonique, sur les bords d'une mer épicontinentale étendue. La source du fer est à rechercher dans un continent situé au Sud, probablement dans la chaîne mobile Pan-Africaine du Nigeria et le Bouclier du Congo.

Ces minerais de fer oolithiques du Sahara Central peuvent être considérés comme une branche importante de la ceinture ferrifère Nord africaine, qui s'étend du Rio de Oro à la Libye.

Краткое содержание

На северо-западе туарегского щита (центральная Сахара, Алжир) располагаются области Bled el Mass, Azzel Mati, Ahnet и Mouydir. Здесь в девонских седиментах установлено 9 горизонтов, содержащих железистые оолиты. Для них являются четыре следующих парагенеза:

$П_1$ = шамозит - магнетит - магхемит - гётит; $П_2$ = шамозит - гематит - гётит - кальцит; $П_3$ = шамозит - гематит - гётит - кварц; $П_4$ = шамозит - гематит - гётит.

Эти 4 типа фаций можно описать так: DFOD - ооиды заключены в матрице из детритного материала; FOND - ооиды заключены в матрице, составленной из не детритного материала; FOC - ооиды спечены; FMC - фаций микроконгломератов.

Ооиды образовались в условиях покоя, в лагунах, или морских бухтах, в результате появления конкреций в седименте из силикатного и богатого железом ила; они стали затем детритом. Вероятно, отложения железистых оолитов явилось результатом повторных стадий седиментации во время девонского периода. Их можно рассматривать, как отменки в циклах отложения. Эти оолитические седименты являются характерными для седиментации у кратонов на краю широкого эпиконтинентального моря. Железо, возможно, происходит из южной части материка, вероятно, из подвижных панафриканских гор Нигерии, или щита Конго - эти руды центральной Сахары могут представлять собой важное ответвление железистого пояса, простирающегося в северной Африке от Rio de Oro до Ливии.

Introduction and geological framework

The Algerian Sahara is located between 7°30'W and 10°E longitude and from 33°N to 19°N latitude. Two Precambrian shields outcrop in the southern part (Touareg Shield) and western part (Reguibat Shield) of this desert area. Paleozoic sediments form a narrow but important belt, 2000 km long, dipping gently northward, and containing fluvial and marine formations.

On the northern part of the Ahaggar (or Touareg) Shield, they constitute the Tassilian Belt (KILIAN, 1922; FOLLOT, 1952; BEUF et al., 1971) composed of the Ahnet, Mouydir and Tassilis N'Ajjer regions (Fig. 1). On the north-western border of the Ahnet and of the Mouydir, the Azzel Matti and the Bled el Mass structures occur.

The four areas: Bled el Mass, Azzel Matti, Ahnet and Mouydir contain numerous ironstone occurrences interbedded within the marine Devonian sediments and are spread over about 150000 sq. kilometers.

Overlying Cambro-Ordovician continental formations and Silurian marine sediments (both about 600 meters thick), the Devonian sediments present thickness and facies variations trending from the north-west to the south-east (Fig. 2).

In the north, the Bled el Mass area is dominated by marine sediments (250 meters thick) which are Lochkovian, Pragian and Emsian in age, are referred to as the Zeimlet, Saheb el Djir and Dkhissa formations and are composed of argillaceous, calcareous and sandy materials, respectively (BOROLLOT et al., 1955; LEGRAND, 1965, 1967; FABRE, 1976).

In the south, the Lower Devonian outcrops in a sinuous cliff called the Outer Tassilis (BIJU-DUVAL et al., 1968). The arenaceous sediments of Asedjrad and Oued Samène Formations (BEUF et al., 1971) indicate a sedimentary zonation in the elementary units from west to east. The unconformities described in the Lower Devonian Ajjers Tassilis (DUBOIS et al., 1967; BEUF et al., 1968, 1970; BENNACEF et al., 1971) have been found again in Ahnet and Mouydir Outer Tassilis.

Marine and continental conditions alternated during sedimentation with the major part of the Lower Devonian consisting of fluvial sandstones. The scattering of palaeocurrent directions suggests that stream discharge of meandering rivers has been irregular, probably seasonal, but always northwest trending. On the other hand, an increase of marine conditions is clearly visible in sediments deposited in the northwest, particularly during the Emsian which was the starting point of a new major transgressive cycle. At that time, the argillaceous-sandy-calcareous sediments of the Azzel Matti Formation were deposited in Azzel Matti and Bled el Mass.

The Middle Devonian commenced with the large Eifelian transgression during which 20–60 meters of shales and limestones of the Meredoua Formation were deposited.

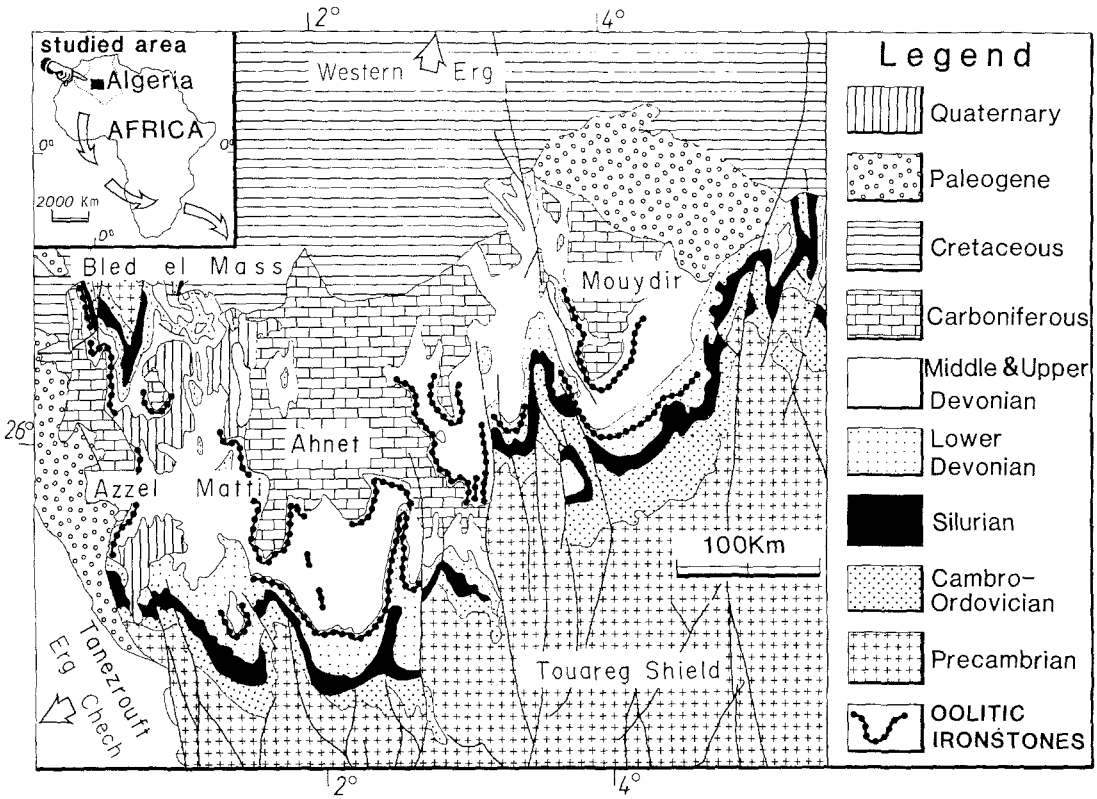

Fig. 1. Geological map of the study area.

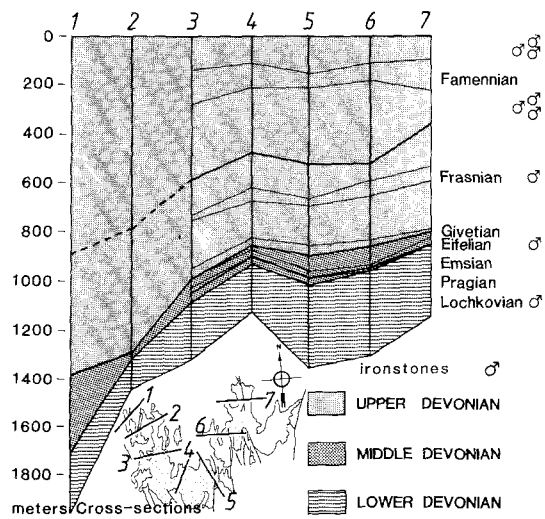

Fig. 2. Variation of Devonian thicknesses from Bled el Mass to Mouydir area (after unpublished data from A. Moussine-Pouchkine).

The subsequent trangression, Givetian in age, deposited 40–100 meters thick sediments constituting the Takoula and In Heguis Formations. Mainly calcareous to the north with numerous reefs (Azzel Matti), they become argillaceous and silty southeastward. These reefs, located directly above old basement faults (Moussine-Pouchkine, 1972) occur within an argillaceous environment.

The Frasnian (200–300 meters) is subdivided into three successive formations: Foum Agam, Imeragen and Meden Yahya (Moussine-Pouchkine, pers. comm.). From bottom to top, calcareous sedimentation decreases and arenaceous deposits increase.

The Early Famennian transgression saw the deposition of 600–700 meters thick of the argillaceous El Ouatiya Formation followed by the silty El Aricha Formation (Moussine-Pouchkine, pers. comm.).

The overlying sandy sediments constitute the Khenig Formation. The Devono-Carboniferous boundary which separates the Khenig Lower sandstones of »Strunien« age from the Khenig Upper

sandstones, of Tournaisian age, is not well known (CONRAD & LEMOSQUET, 1984).

The Carboniferous (about 1800 meters) can be subdivided into several cycles resulting largely from eustatic variations (FABRE & MOUSSINE-POUCHKINE, 1971).

Finally, the northward trending Cretaceous and Pliocene »Hamada« cover overlies the Palaeozoic rocks. All these formations are covered by the extensive sand dune fields of the Western Erg and the Erg Chech.

The geological record, particularly for Devonian sediments, indicates a close relationship between sedimentation and epeirogenic movements, especially for those movements which were synchronous with the Acadian orogeny, which developed since late Silurian times and allowed a lateral sedimentary progradation northwestward. Previous to the Acadian orogeny, some basement movements highlighted major structural directions such as the Foum Belrem axis. Since the Cambro-Ordovician, tectonic movements have resulted in the isolation of several basins, e.g. Ahnet and Mouydir.

This process subsequently continued and a general northwestward slope initiated a multipulsed sedimentation. The Hercynian orogeny (Variscan Orogeny of DONZEAU et al., 1982) which followed the Acadian orogeny, resulted in folding of this part of the Saharan Platform.

The oolitic ironstones

Occurrence

Within the Devonian sediments, nine ironstone occurrences of different thickness are allocated to the Lochkovian, Eifelian, Frasnian and Famennian (Fig. 3). Detailed cross-sections through the study area, show the distribution in time of the ironstones. Table 1 indicates the thickness of the oolitic ironstones, indexed 1 to 9, from bottom to top in the stratigraphic column. The oolitic ironstones are of the EXID type (Extensive Ironstone Deposition) extending over several tens to hundreds of kilometers (Fig. 4.a. b. c.). This type contrasts with the LOID type (Local Ironstone Deposition) previously defined for the oolitic ironstones of the Saharan Platform (GUERRAK, 1987).

Ironstones of the study area are very similar to the »Oolitic Minette« type of ROUTHIER (1963) and to the »Clinton« type of GROSS (1965). In another classification, they are similar to the SCOS-IF type (sandy, clayey and oolitic, shallow-inland-sea iron formation: KIMBERLEY, 1978, 1981).

AGE	IRONSTONES	THICKNESS (meters)
	9	3.5
	8	1.2
	7	2.0
Famennian	6	1.0
	5	4.5
	4	0.8
Frasnian	3	5.0
Eifelian	2	4.0
Lochkovian	1	0.8
	Total	22.8

Tab. 1. Thickness of oolitic ironstone beds.

Mineralogical composition

The ironstones can be subdivided into four types of paragenetic associations P1, P2, P3, P4, as shown in Table 2, P3 and P4 being the most widespread.

Whereas hematite and goethite are common in Phanerozoic ironstones, chamosite which is a 14 Å trioctahedral chlorite (BAYLISS, 1975; BAILEY, 1980) is very frequent in Paleozoic ironstones of the Saharan Platform (GUERRAK, 1987), and especially in the deposits of the study area. It has been often confused with berthierine (7 Å trioctahedral serpentine).

Chamosite appears widespread within ooliths and groundmass, as nuclei, as intraclasts or as the major component of the whole oolith. Hematite, strictly related to chamosite, or concentrically alternating within the layers of ooliths, results in the centrifugal increase of the chamosite oxidation and occurs in all the ironstone: nucleus, matrix and layers.

To our knowledge, the Azzel Matti ironstone is the only EXID type on the Saharan Platform reported to contain magnetite. Here magnetite, overlying chamositic-hematitic ironstone, seems to be due to

Fig. 3. Distribution of ironstone through Devonian formations. ▶

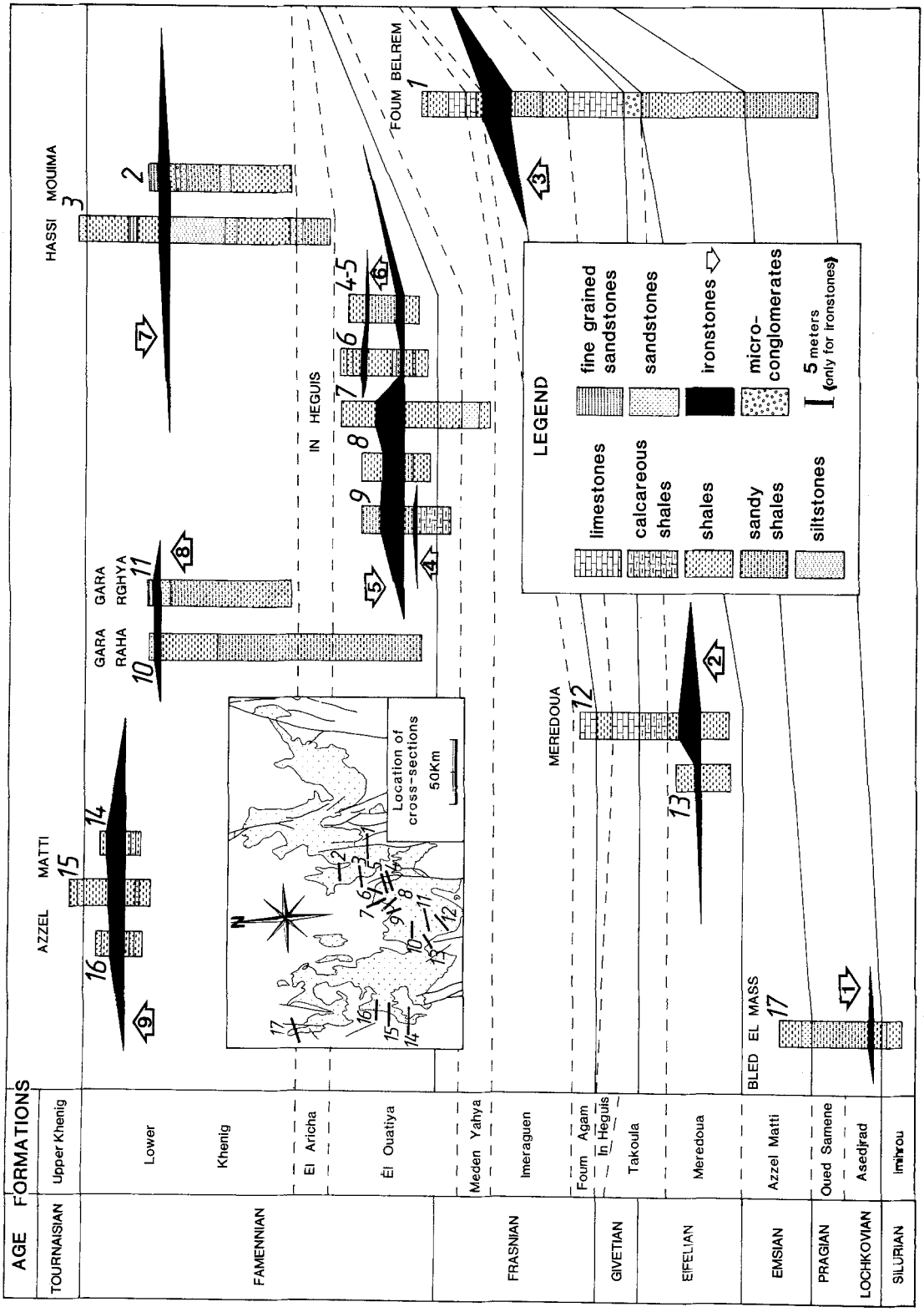
AGE
FORMATIONS
TOURNAISIAN
Upper Khenig
FAMENNIAN
Lower
Khenig
El Aricha
El Ouatiya
FRASNIAN
Meden Yahya
Imeraguen
GIVETIAN
Foum Agam
In Heguis
Takoula
EIFELIAN
Meredoua
EMSIAN
Azzel Matti
PRAGIAN
Oued Samene
LOCHKOVIAN
Asedjrad
SILURIAN
Imihrou
AZZEL MATTI
HASSI MOUIMA
GARA RAHA
GARA RGHYA
IN HEGUIS
FOUM BELREM
MEREDOUA
BLED EL MASS
Location of cross-sections
50Km
N
LEGEND
limestones
calcareous shales
shales
sandy shales
siltstones
fine grained sandstones
sandstones
ironstones
micro-conglomerates
5 meters (only for ironstones)

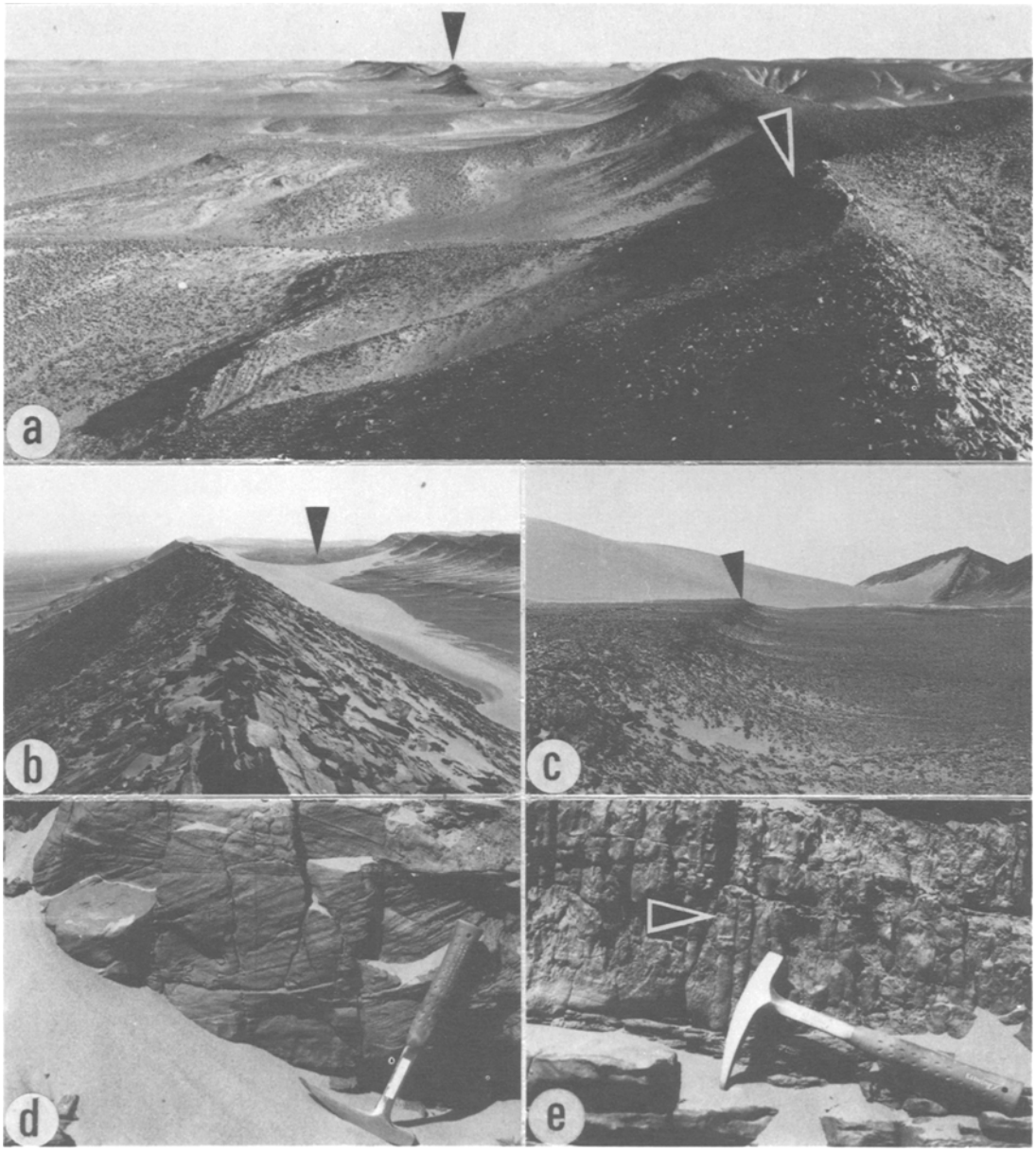

Fig. 4. (a-e). a: General view of a typical ironstone of EXID type (In Heguis, area). b-c: Hassi-Mouima: the ironstone bed number 7. d: Gara Raha: herringbone structures in the ironstone. e: Skolithos burrows well preserved within the ironstone.

local chemical conditions of iron deposition, at the beginning of deepening of the microbasin where ironstone was deposited. It could be linked to an increase of organic matter within the sea water during the more advanced stage of diagenesis (named locomorphic by DAPPLES, 1967). According to HAN (1986) this discharge of organic matter allows the decrease of oxidation-reduction potential and the increase of pH. The slow percolation of these reducing and basic waters within a porous ironstone could induce the transformation of hematite (previously resulting from differential oxidation of chamosite)

PARAGENESES	INDEX	IRONSTONE BEDS
chamosite-hematite goethite	P_4	1-2-5-7-8-9
chamosite-hematite goethite-quartz	P_3	4-5-6
chamosite-hematite goethite-calcite	P_2	3
chamosite-magnetite maghemite-goethite	P_1	9

Tab. 2. Distribution of paragenetic associations within the oolitic ironstone.

into magnetite. Maghemite occurs as the main weathering product of magnetite (in meteoric conditions), martite having been never detected. This is confirmed by chemical analyses (Table 6) showing a very low concentration of FeO in the magnetitic ironstone. Hematite can probably be considered as a synsedimentary mineral induced by the transformation of chamosite. We also described the same phenomenon for Mecheri and Gara Djebilet deposits (GUERRAK & CHAUVEL, 1985). Goethite is the typical mineral of weathering processes, typically formed under oxidizing conditions at ordinary temperatures and pressures. It occurs with hematite and can completely replace it. So, goethite appears as the last oxidized mineral of the oolitic ironstone, and cannot be directly produced by chamosite.

Calcite, when it is present (e.g. Foum Belrem), is generally a secondary mineral. It appears to be replacing chamosite and hematite. It can also occur as the main constituent of bioclasts.

Quartz, as detrital grains or oolith nuclei, is not very widespread: it mainly occurs in the detrital and microconglomeratic ironstone facies. Very rare rutile grains have been found acting as nuclei but never within the matrix. Apatite is especially present as intraclasts within practically all the ironstone facies, and very rarely as nuclei. It could again occur as microinclusions within ferriferous minerals.

Textural characters

Four main ironstone facies have been defined on the basis of systematic petrographical analyses:

(i) a facies containing ooliths scattered in a detrital groundmass (FOD); (ii) a facies with ooliths scattered in a non-detrital groundmass (FOND); (iii) a facies with cemented ooliths and pore-filling structure (FOC); and (iv) a microconglomeratic facies (FMC).

These ironstone facies reflect the history of the oolitic sediment. After accretion mechanisms related to intrasedimentary processes, and several periods of suspension and deposition, took place a peculiar oolitic ironstone facies formed. The microconglomeratic facies (FMC) and the detrital facies (FOD) could be related to a final deposition within a high energy environment, whereas non-detrital (FOND) and cemented facies (FOC) could be related to quiet water conditions of the final period of sedimentation.

The variations in the mineralogical composition of ooliths allow the distinction of sub-facies.

Fig. 5 shows the distribution of ferriferous facies within the different ironstone beds and emphasizes the detailed mineralogy of nuclei, cements and groundmasses.

The main ferriferous facies are vertically distributed as indicated in Table 3. The FOND facies is the widespread one, with a total thickness of about 12.3 meters. FOD and FOC facies, respectively contain 5.2 meters and 5.3 meters of ironstone deposited during Devonian times.

The FMC facies, only located at the top of Bed 5, is 0.5 meter thick. The textural characteristics are as follows:

(i) generally, ooliths are very abundant, particularly within FOD and FOC facies, occurring separately (Fig. 6.d) or as nuclei of other ooliths (Fig. 6.e); (ii) in some examples, early stages of fragmentation where ooliths are completely crushed by detrital grains, are well preserved, e.g. in the Meredoua area; (iii) »complex ooliths« or »multiple ooliths« (Fig. 6.a.

AGE	IRONSTONE BEDS	IRONSTONE FACIES	PARAGENESES
	9	FOC (FOND)	P_1 - P_4
	8	FOD (FOND-FOC)	P_4
Famennian	7	FOND (FOC)	P_4
	6	FOC	P_3
	5	FOND (FMC-FOC)	P_3 - P_4
	4	FOC	P_3
Frasnian	3	FOND	P_2
Eifelian	2	FOD	P_4
Lochkovian	1	FOND	P_4

Tab. 3. Distribution in time of ironstone facies and parageneses (FMC = microconglomeratic facies, FOD = detrital facies, FOND = non detrital facies, FOC = cemented facies).

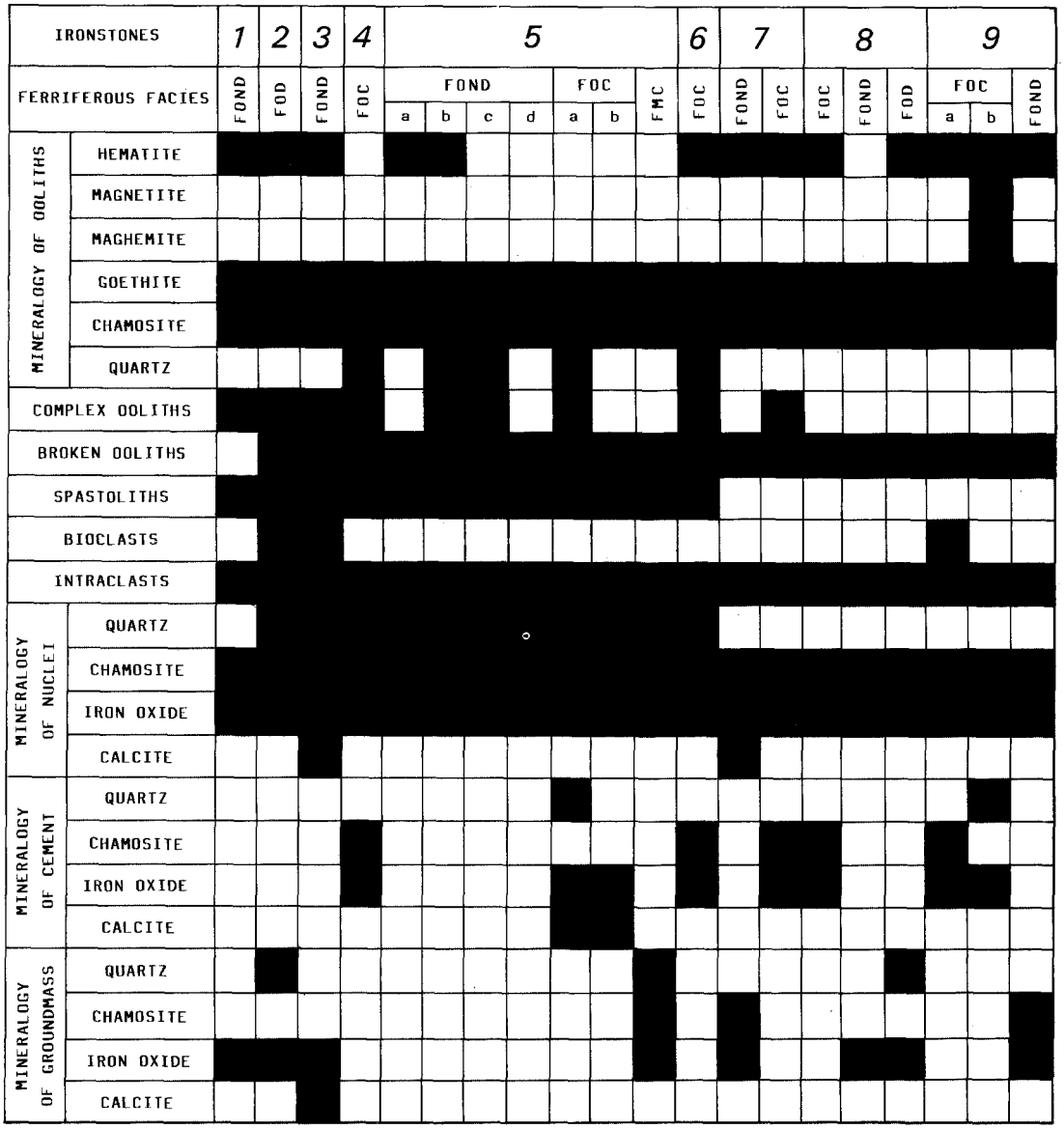

Fig. 5. Petrographical and mineralogical composition of the oolitic ironstone.

b. c.) formed by accretion around several ooliths, occur especially within the FOC facies, which appears to be the most evolved oolitic ironstone facies; (iv) many ooliths are distorted (spastoliths, Fig. 6.f). Flattened or only slightly deformed, they can be associated with »normal ooliths« or concentrated in some peculiar facies. Originally composed of chamosite, they probably have been deformed when they were still in a plastic stage. Within such spastoliths, nuclei could consist of chamosite, hematite or quartz. When the nucleus was chamositic, it was also deformed and various shapes appeared.

The size range of ooliths is 160 μm to 1800 μm. The biggest ooliths occur in Foum Belrem area (FOND facies with calcitic matrix), the smallest in In Heguis area (FOND facies with oxidized matrix).

These observations indicate the lack of direct relationships between the facies and the size of ooliths. The coarseness of ooliths seems to be dependent on the accretion rapidity and on the frequency of alternating accretion and reworking periods.

This emphasizes differences between the primary oolitization environment and the final ironstone deposit.

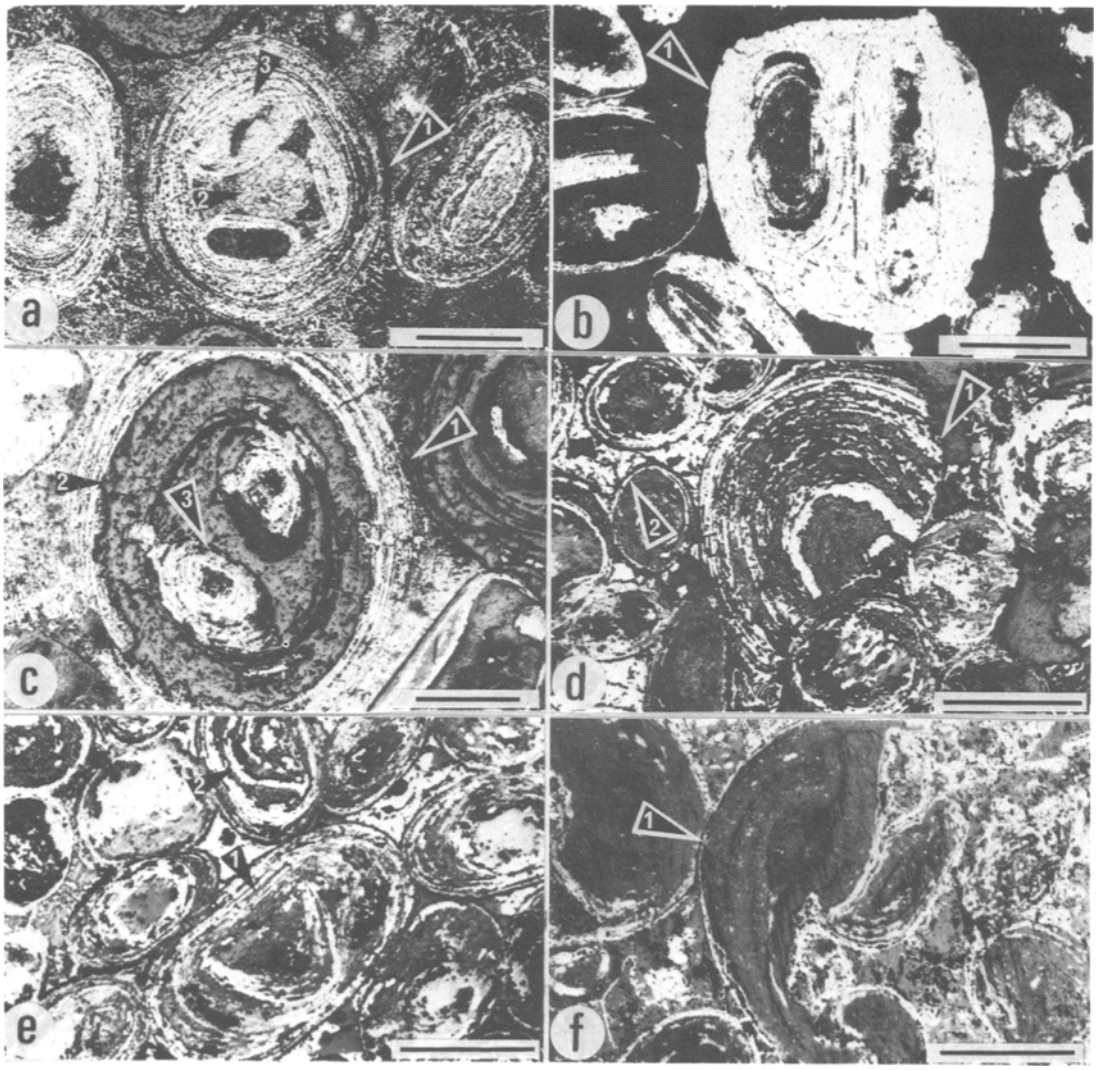

Fig. 6. (a-f). a: Ironstone bed 6 (In Heguis); reflected light. A complex oolith (in a FOC facies is composed by three hematitic-chamositic ooliths (3) around a central goethitic intraclast (2). Layers are alternating chamositic-hematitic (1). Scale bar is 150 μm. b: Ironstone bed 6 (In Heguis); transmitted light. A complex oolith (FOC facies) is composed by two goethitic ooliths replaced by amorphous silica (1). Scale bar is 250 μm. c: Ironstone bed 6 (In Heguis); reflected light. A complex oolith is composed by two hematitic-goethitic ooliths (3) surrounded by chamositic (2) and hematitic layers (1). Scale bar is 150 μm. d: Ironstone bed 9 (Azzel Matti); reflected light. A chamositic-hematitic oolith (1) is included within a FOC facies cemented by chamosite (grey) and goethite (white). A pore filling structure is well developed in (2). Scale bar is 100 μm. e: Ironstone bed 9 (Azzel Matti); reflected light. Two broken chamositic-goethitic ooliths (1) and (2) are used as nuclei of other ooliths: FOC facies with pore-filling structure. Scale bar is 100 μm. f: Ironstone bed 1 (Bled el Mass); reflected light. A chamositic spastolith (1) oxidized in the cortex (white) is included in a chamositic-goethitic matrix (FOND facies). Scale bar is 100 μm.

Sedimentological paleoenvironment

Methodology

The sedimentological study, using Markov chain analysis (Krumbein & Dacey, 1969; Selley, 1970; Allen, 1974; Harms et al., 1982), was successefully applied to ironstone sedimentation by Guerrak & Chauvel (1985) in the case of a LOID type deposit (Local Ironstone Depositon). This method is used in the present paper because of the difficulty of making

coherent correlations over such a large area and of interpreting the sedimentological features of the ironstone deposits. The main interest of this analytical study is to define the vertical arrangement of facies in sedimentary sequences, using relatively little data.

	A	B	C	D	E	F	G	H	I	TOTAL
A	-	-	1	-	-	-	1	-	1	3
B	1	-	1	2	-	5	10	-	-	19
C	1	2	-	-	2	1	9	-	-	15
D	-	-	-	-	-	-	1	-	-	1
E	1	1	-	-	-	-	2	-	-	4
F	-	3	4	-	-	-	4	-	-	11
G	-	12	13	1	2	2	-	1	2	33
H	-	1	-	-	-	-	-	-	1	2
I	-	-	-	-	-	-	3	-	-	3
TOTAL	3	19	19	3	4	8	30	1	4	91

OBSERVED NUMBER OF TRANSITIONS BETWEEN FACIES

	A	B	C	D	E	F	G	H	I	TOTAL
A	0.10	0.63	0.63	0.10	0.13	0.26	0.99	0.03	0.13	3
B	0.63	3.97	3.97	0.63	0.83	1.67	6.26	0.21	0.83	19
C	0.49	3.13	3.13	0.49	0.66	1.32	4.94	0.16	0.66	15
D	0.03	0.21	0.21	0.03	0.04	0.09	0.33	0.01	0.04	1
E	0.13	0.83	0.83	0.13	0.17	0.35	1.32	0.04	0.17	4
F	0.36	2.30	2.30	0.36	0.48	0.97	3.63	0.12	0.48	11
G	1.09	6.89	6.89	1.09	1.45	2.90	10.88	0.36	1.45	33
H	0.06	0.42	0.42	0.06	0.09	0.17	0.66	0.02	0.09	2
I	0.10	0.63	0.63	0.10	0.13	0.26	0.99	0.03	0.13	3
TOTAL	3	19	19	3	4	8	30	1	4	91

TRANSITION PROBABILITIES FOR RANDOM SEQUENCE

	A	B	C	D	E	F	G	H	I
A	-0.10	-0.63	0.37	-0.10	-0.13	-0.26	0.01	-0.03	0.87
B	0.37	-3.97	-2.97	1.37	-0.83	3.33	3.74	-0.21	-0.83
C	0.51	-1.13	-3.13	-0.49	1.34	-0.32	4.06	-0.16	-0.66
D	-0.03	-0.21	-0.21	-0.03	-0.04	-0.09	0.67	-0.01	-0.04
E	0.87	0.17	-0.83	-0.13	-0.17	-0.35	0.68	-0.04	-0.17
F	-0.36	0.70	1.70	-0.36	-0.48	-0.97	- 0.37	-0.12	-0.48
G	-1.09	5.11	6.11	-0.09	0.55	-0.90	-10.88	0.64	0.55
H	-0.06	0.58	-0.42	-0.06	-0.09	-0.17	- 0.66	-0.02	0.91
I	-0.10	-0.63	-0.63	-0.10	-0.13	-0.26	2.01	-0.03	-0.13

OBSERVED MINUS RANDOM TRANSITION PROBABILITIES

Tab. 4. Matrix analysis of sedimentary data.

The recording of the boundaries between the different facies in each formation, allows the definition of nine distinct lithofacies: A = conglomerate, B = oolitic ironstone, C = sandstone, D = fine-grained sandstone, E = siltstone, F = sandy shale, G = shale, H = calcareous shale, I = limestone. These facies can be schematically described as follows:

(i) A: poorly developed, conglomerates are commonly clast supported with basal normal grading. Particle size ranges between 0.2 and 6 mm. They can be classified as granules-conglomerates. Well rounded, clasts are composed of sandstones, siltstones, mudstones and calcitic bioclasts, cemented by a calcareous or a sandy matrix. (ii) B: macroscopically, oolitic ironstones consist of normal and microconglomeratic ironstones. (iii) C: sandstones commonly green, grey or brown in color, are composed of well rounded quartz grains, which are dominant, with scarce lithic grains in a chloritic to ferruginous cement. They can be classified as mature sandstones. (iv) D: fine sandstones green or brown in color, are rocks composed intirely of well rounded quartz grains cemented by more or less oxidized chlorite. (v) E: siltstones have the same composition as sandstones and are only different in grain size. (vi) F: grey to brown in color, sandy shales mostly consist of shales containing discontinuous sandy layers. (vii) G: shales are the most abundant facies and occur in all the sections. They are mainly composed of green clay minerals, essentially chlorites, more or less weathered. Their color can be green, grey, purple or red, depending on the degree of alteration. (viii) H: calcareous shales. There is a progressive transition between shales and limestones, resulting in the development of calcareous inclusions and paches. (ix) I: bleu or grey in color, the massive limestones occur in two areas (Foum Belrem and Meredoua) and are highly fossiliferous, especially containing brachiopods and goniatites.

The calculation of predicted matrix (Table 4) allows one to draw a facies relationship diagram (Fig. 7.a) which records the most probable transi-

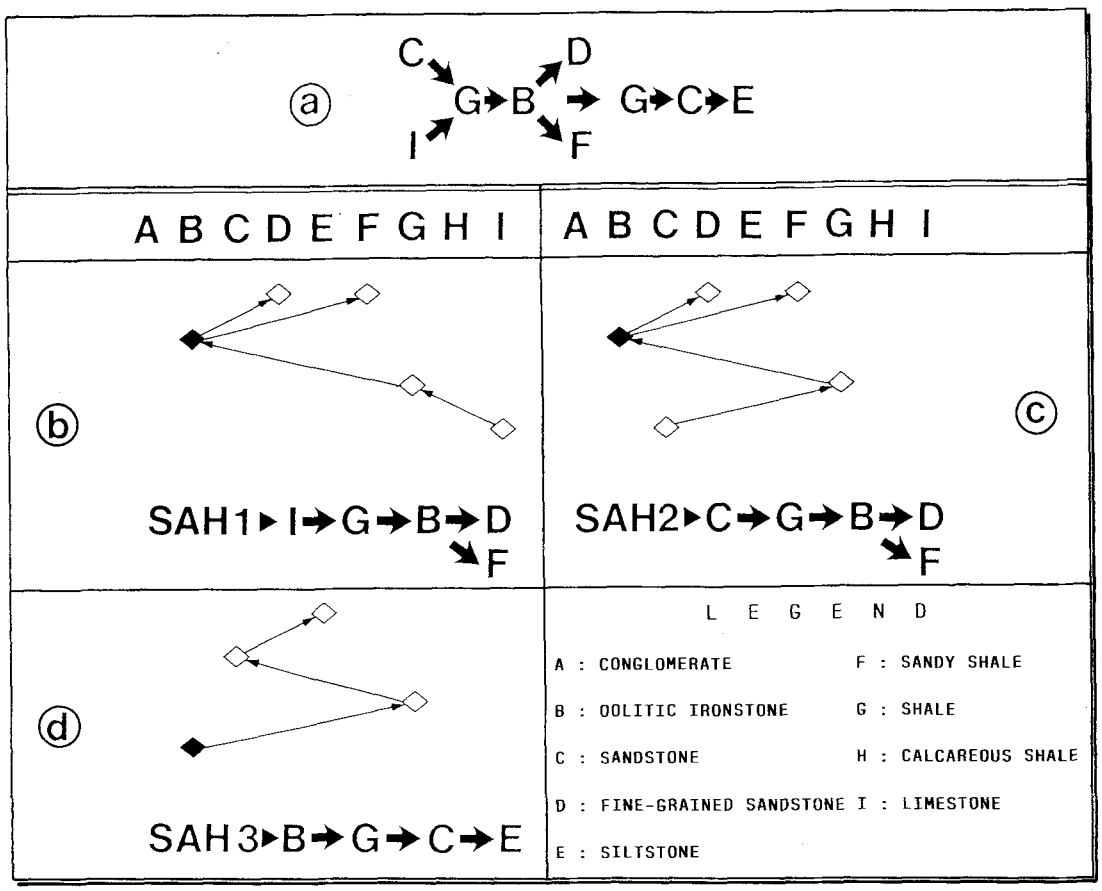

Fig. 7.a: Facies relationships diagram. b-c-d: sequential evolution of the different facies.

tions. Three sedimentary sequences, SAH. 1, SAH. 2, SAH. 3, (Fig. 7.b. c. d.) are deduced.

In both SAH. 2 and SAH. 3 sequences, facies are argillaceous to sandy, the SAH. 1 being calcareous to argillaceous.

The ironstone is located:

(i) within SAH. 1 and SAH. 3: in a transition zone, between a coarsening and a fining-upwards sequence (top of a regressive cycle), and (ii) within SAH. 2, at the bottom of a fining-upwards sequence (transgressive cycle).

The distribution of SAH. 1, SAH. 2 and SAH. 3 through the geological formations (Fig. 8), suggests vertical successions with two main trends appearing:

(i) Lochkovian → Eifelian → Frasnian

(ii) Frasnian → Famennian, with internal pulses.

The comparison between this evolution and the ironstone facies distribution shows a parallel behaviour, with the exception of ironstone deposits 3 and 4. This seems to be related to the textural evolution and the nature of the sequence (transgressive or regressive).

Sedimentary structures and morphology

Numerous sedimentary structures have been recorded in the ironstone:

(i) tabular cross-beddings, sometimes of large amplitude, (ii) herringbone structures (Fig. 4.d) (1–1.5 m), (iii) channels, (iv) vertical burrows of different length (10–30 cm) related to *Skolithos ichnogenus* (GUERRAK, unpublished data; Fig. 4.e). They can be widespread (e.g. Djebel Hassi Mouima) where the hanging wall of the ironstone is entirely perforated by numerous burrows.

Locally (e.g. Meredoua area), well preserved brachiopod shells are present (e.g. *Paraspirifer cultrijugatus:* MOUSSINE-POUCHKINE, unpublished data).

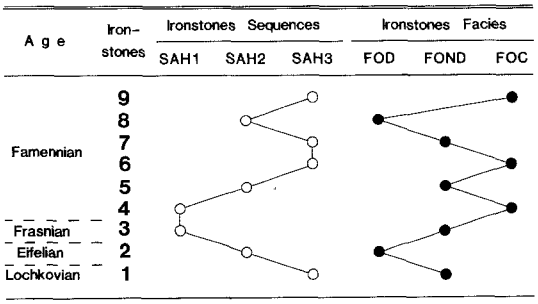

Fig. 8. Distribution in time of sedimentary sequences and ironstone facies.

Although ironstone occurred as extensive beds, their thicknesses are not always constant. Variations have been observed between cross-sections and from one locality to another, showing a more or less lenticular aspect related to the topography of the paleoenvironment.

Interpretation

The oolitic ironstone sedimentation forms an important part of the sedimentary cycles of the Devonian. Each large sedimentary cycle was not continuous but appears to be made up of many small cycles. The evidence for such pulses is found in the oolitic ironstone deposition, similar to that described in Ordovician sediments of the Ougarta Ranges area in the western Sahara.

In the Ahnet, Azzel Matti and Bled Mass areas, the cycles were controlled by eustatic rise and fall of sea level or by epeirogenic movements.

BERTRAND-SARFATI et al. (1977) have suggested a link between oolitic sedimentation of the north-western border of the Touareg Shield, and marine transgressions. HALLAM & BRADSHAW (1979) related ironstones to falling sea level (regressions) for the NW European Jurassic. VAN HOUTEN & BHATTACHARYYA (1982) suggest that Phanerozoic ironstones were fostered by widespread transgressions and decrease of detrital influx into shallow seas flooding cratonic or intracratonic basins.

In accordance with suggestions of VAN HOUTEN & BHATTACHARYYA (1982), our opinion is that ironstones were mainly deposited during the transition between transgressive and regressive cycles, during a period of relative tectonic stability.

At the scale of the Saharan area, the marine Paleozoic sedimentation would have involved large, flat, quiet and constant epicontinental environments as described by BERTRAND-SARFATI et al. (1977), BUROLLET & BUSSON (1983), and LEGRAND (1985). This explains the large regional extension of EXID type deposits.

While the large Silurian transgression and the Permo-Carboniferous transgressions and regressions were probably caused largely by eustatic variations (FABRE & MOUSSINE-POUCHKINE, 1971), the Devonian regressions and transgressions of the Ahnet basin and limitroph areas were dominated by epeirogenic movements (BERTRAND-SARFATI et al., 1977). The main argument for this hypothesis is the development of the northwestward subsidence, in the direction of the Saoura (MENCHIKOFF, 1957). This subsidence is evident laterally and vertically in Devonian marine sediments which thicken towards the

Ougarta Ranges. This could explain the decrease of the oolitic ironstone deposition northwestward, where both rapid subsidence and rapid deposition gradually changed to a slow epicontinental sedimentation. Therein, we can note the lack of ironstones in the Devonian thick sediments of Ougarta Ranges. However, the extensive distribution of the oolitic ironstones (EXID type) in the Ahnet area could be the product of multiple processes. These processes which were likely of an eustatic origin, could have been disturbed by epeirogenic movements. The oscillations of sea level were probably supplemented by »local« tectonic effects, particularly revealed by the irregularity of the ironstone deposits (thickness and granulometry). VAN HOUTEN (1985) and more recently, MAYNARD (1986), related oolitic ironstones to periods of high sea level and dispersed cratonic areas.

In the area discussed by this paper, we have tried to quantify the oolitic ironstone sedimentation in terms of the duration through Devonian times. Fig. 9 shows the increase of frequency of the oolitic ironstone during Devonian times. Therefore we were able to define »Oolitic Ironstone Preservation Amounts« for each period, and to estimate the ironstone thickness deposited per million years. Nevertheless, one must realize that these amounts have been obtained without taking into account possible compaction or hiatuses of deposition, or erosion.

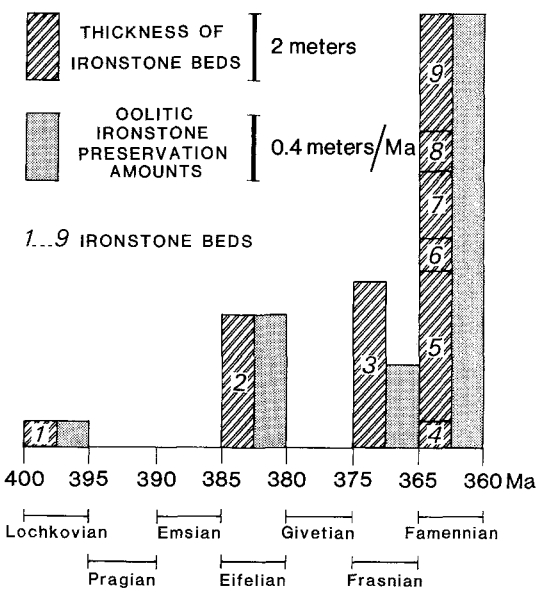

Fig. 9. Distribution of ironstone thicknesses and Oolitic Preservation Amounts through Devonian times (Ages after geochronological data from ODIN & GALE, 1982).

This oolitic ironstone sedimentation is proportional to the deposition of argillaceous and silty materials. Over the very flat shelves bordering the paleocontinent of Gondwanaland, ironstones began to develop as chamositic sediments in tranquil zones (JAMES & VAN HOUTEN, 1979; VAN HOUTEN & PURUCKER, 1984) such as lagoons or embayments. Flat barrier island systems or sand ridges could occur parallel to the coast, leaving some connections with the open sea. This tranquil but continuously submerged area of ironstone deposition, can be considered as a provisional source for the occurrence of the ooliths.

Broken ooliths, centrifugal and concentric oxidation of the layers and the formation of multiple ooliths, demonstrate the detrital nature of the ooliths and of the beds formed between successive accretionary environments. In some cases, the energy level could have been fairly important in the ironstone deposition (i.e. tabular cross-beddings of high amplitude).

Sometimes, herringbone structures indicate an intertidal environment for the ironstone. A tidal control of oolitic sedimentation has previously been suggested by TEYSSEN (1984) for the Jurassic minette of Luxembourg and Lorraine.

Geochemistry of oolitic ironstones

Analytical Procedure

Thirty-six samples of different types of oolitic ironstones (Table 5) were selected from the less weathered outcrops and analyzed for major and some trace elements (Bi, Co, Cr, Cu, F, Ni, Pb, Zn; Table 6).

About 100 g of crushed material were ground to a fine powder in a tungsten carbide mill (for major elements) and in an agate ball mill (for trace elements).

The methods used and their detection limits are presented in Table 7. The Atomic Absorption Spectrophotometer used was a Perkin-Elmer 403. However, for some trace elements, the results have been rounded by the laboratory, indicating that these results are partly semi-quantitative.

The multi-element correlations and linear regressions were calculated using a microcomputer Hewlett-Packard 98–45 B.

Composition

The distribution of the elements, as shown in Fig. 10, enables the recognition of three geochemical types of oolitic ironstones (OIS), namely Fe-poor, Fe-rich and Ca-rich types.

location of cross-sections	Corresponding ironstone beds	Number of samples
1. Foum Belrem	3	2
2. Hassi Mouima	7	2
3. Hassi Mouima	7	2
4. In Heguis	6	1
5. In Heguis	6	1
6. In Heguis	6	2
4. In Heguis	5	1
5. In Heguis	5	1
6. In Heguis	5	1
7. In Heguis	5	2
8. In Heguis	5	2
9. In Heguis	5	2
10. Gara Raha	8	2
11. Gara Rghya	8	2
12. Meredoua	2	2
13. Meredoua	2	2
14. Azzel Matti	9 & 9'	3
15. Azzel Matti	9	2
16. Azzel Matti	9	2
17. Bled El Mass	1	2
	Total of samples	36

Tab. 5. Chemical analyses: location of oolitic ironstone samples (according to Fig. 3).

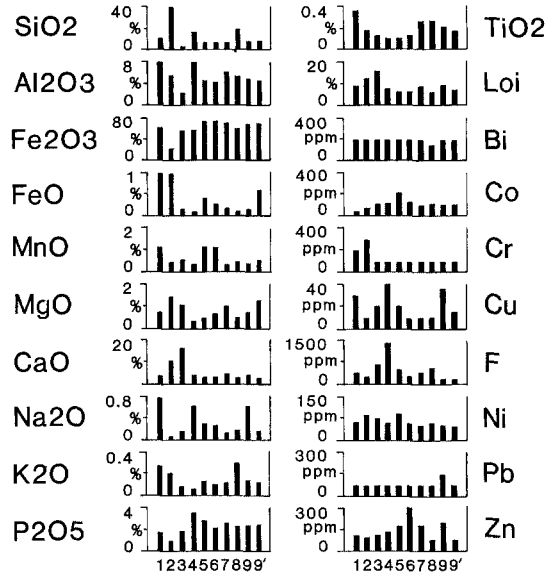

Fig. 10. Average distribution of major and minor elements for the oolitic ironstone beds number 1 to 9 (9' is the magnetitic ironstone).

(i) Fe-poor ironstones: this type is represented by the OIS2, located in the Meredoua area. It contains least amounts of iron with Total Fe being 18.77%; SiO2 content is 42.50%. This can be considered as an oolitic sandstone rather than a pure oolitic ironstone. The relatively high value of CaO, when compared to Ca-rich ironstone, can be related to calcitic bioclasts, particularly of Brachiopods. Compared to the other geochemical types, phosphorus is very low, with $P_2O_5 < 1\%$.

(ii) Ca-rich ironstones: OIS.3 of Foum Belrem area is fairly rich in calcite (16.92% CaO). This is a function of its occurrence within an argillaceous to calcareous dominated sequence.

(iii) Fe-rich ironstones (OIS 1, 4, 5, 6, 7, 8, 9): these OIS reveal a range of Fe_2O_3 varying from 56.32% to 74.40%. FeO is very low with 0.05–0.37% and P_2O_5 rather high: 1.85–3.58%. P_2O_5 concentration is commonly proportional to Fe_2O_3 content in the Saharan ironstones. This is due to the presence of apatite as microinclusions within chamosite, hematite and goethite.

Nevertheless, it must be noted for these three groups that the chemical composition has likely been modified by weathering. Consequently the enrichment in iron can be partly induced by secondary conditions developed after the deposition.

Linear correlations

Positive and negative multi-elements linear correlations have been calculated but only values of correlation coefficients r greater than 0.5 have been represented in Table 8. On the other hand, the most significant values of r are those greater than 0.75.

The main oxides of the ironstone are SiO_2 and Fe_2O_3. There is an inverse correlation between the two which is a common feature in the ironstones. However, the Meredoua ironstone (bed 3) is exception to this rule.

The positive correlation of FeO and Cr is explained by the similar behavior of Fe^{++} and Cr^{+++} which are commonly concentrated in clays (WEDEPOHL, 1974).

CaO after Loss on Ignition commonly shows a positive correlation, whereas the correlation between Na_2O and Cu cannot be interpretated because of the very low values of sodium. This also is the case for the negative correlation of K20/Bi.

%	(1)	(2)	(3)	(4)	(5)	(6)	(7)	(8)	(9)	(9')	Average	Range		CONTINENTAL CRUST
SiO_2	11.50	41.50	4.10	18.50	7.37	6.15	7.95	20.00	7.65	7.85	13.26	4.10	41.50	61.9
Al_2O_3	8.12	5.72	2.43	7.93	4.73	4.41	6.04	5.78	5.02	4.66	5.48	2.43	8.12	15.6
Fe_2O_3	62.50	24.50	56.40	56.32	73.27	74.40	69.15	60.10	68.85	72.00	61.75	24.50	72.00	2.6
FeO	1.22	2.12	0.11	0.05	0.37	0.18	0.14	0.05	0.08	0.66	0.50	0.05	2.12	3.9
MnO	1.23	0.58	0.71	0.39	1.24	1.19	0.35	0.58	0.45	0.68	0.74	0.35	1.24	0.1
MgO	0.69	1.36	1.05	0.30	0.44	0.63	0.83	0.50	0.74	1.26	0.78	0.30	1.36	3.1
CaO	3.84	11.32	16.92	3.89	3.04	3.21	4.55	3.19	5.15	2.89	5.80	2.89	16.92	5.7
Na_2O	0.79	0.06	0.18	0.64	0.31	0.29	0.12	0.19	0.60	0.19	0.34	0.06	0.79	3.1
K_2O	0.27	0.20	0.09	0.06	0.13	0.10	0.12	0.30	0.15	0.13	0.15	0.06	0.30	2.9
P_2O_5	1.85	0.98	1.94	3.58	2.92	2.25	2.64	2.44	2.51	2.54	2.36	0.98	3.58	0.3
TiO_2	0.36	0.18	0.12	0.10	0.10	0.12	0.28	0.28	0.21	0.18	0.19	0.10	0.36	0.8
LOI	8.32	12.23	15.98	8.21	6.40	6.77	8.03	6.24	8.33	7.23	8.77	6.24	15.98	
Total	100.69	100.75	100.03	99.97	100.32	99.70	100.20	99.65	99.74	100.27	100.13			100
ppm														
Bi	200	200	200	200	200	200	200	150	200	200	195	150	200	0.06
Co	40	80	120	120	220	130	100	125	115	115	116	40	220	29
Cr	200	300	100	100	100	100	100	100	100	100	130	100	300	185
Cu	30	10	20	40	20	10	10	10	35	15	20	10	40	75
F	600	400	1000	1500	775	450	600	800	300	300	672	300	1500	700
Ni	80	120	100	80	132	80	70	80	65	65	87	65	132	105
Pb	100	100	100	100	100	100	100	100	200	100	110	100	200	8
Zn	100	250	100	230	305	220	175	140	130	155	180	100	305	80

Tab. 6. Average chemical analysis of ironstone beds (9')is the magnetitic oolitic ironstone of Azzel Matti.

Oxides & Elements	Analytical Method	Detection limits in ppm
SiO_2	Colorimetry	500
Al_2O_3	Colorimetry	500
Fe_2O_3	Colorimetry	500
FeO	Volumetry	500
MnO	Atomic absorption spectrophotometry	500
MgO	Atomic absorption spectrophotometry	500
CaO	Atomic absorption spectrophotometry	500
Na_2O	Flame photometry	100
K_2O	Flame photometry	100
TiO_2	Colorimetry	100
P_2O_5	Colorimetry	100
LOI	Gravimetry	500
Bi	Atomic absorption spectrophotometry	100
Co	Atomic absorption spectrophotometry	40
Cu	Atomic absorption spectrophotometry	20
Cr	Atomic absorption spectrophotometry	40
Ni	Atomic absorption spectrophotometry	100
Pb	Atomic absorption spectrophotometry	100
Zn	Atomic absorption spectrophotometry	20
F	Potentiometry	100

Tab. 7. Analytical methods and detection limits (after EREM Laboratory).

	CORRELATION COEFFICIENTS (r> 0.5)
SiO_2	Fe_2O_3 (-0.88), FeO (0.54), K_2O (0.52), Cr (0.63)
Al_2O_3	Cu (0.58)
Fe_2O_3	FeO (-0.52), CaO (-0.60), P_2O_5 (0.54), LOI (-0.59), Cr (-0.66)
FeO	P_2O_5 (-0.51), Cr (0.76)
MnO	P_2O_5 (-0.53)
CaO	LOI (0.95)
Na_2O	Cu (0.75), Pb (0.51)
K_2O	TiO_2 (0.68), Bi (-0.82)
TiO_2	Zn (-0.61), Bi (-0.63)
P_2O_5	Co (0.55), Cr (-0.52)
Ni	Co (0.81), Zn (0.80)
Co	Zn (0.71)
Cu	Pb (0.74)

Tab. 8. Main correlation coefficients.

Ni versus Co and Zn, presents a good correlation which can be related to their similar ionic radii.

Comparison with crustal abundance

The comparison of the mean chemical composition of the ironstones of the study area and the bulk composition of the crust (Table 6, Fig. 11) has been made on the basis of anhydrous analyses. The data of the crustal abundance used in the present paper are those reported by RONOV & YAROSHEVSKY (1969) for major elements and by TAYLOR & MCLENNAN (1985) for trace elements. This comparison highlights the following aspects:

(i) the enrichment of Fe203 was probably increased by weathering processes and this is very common for ironstone deposits;

(ii) the behaviour of MnO is closely linked to Fe203, the geochemistry of iron and manganese being very similar. Therefore, with an increasing in iron, an enrichment in manganese can be expected. However, a high Fe/Mn ratio exists within the ironstones (KRAUSKOPF, 1957) and a complete separation of manganese and iron has been recorded in numerous deposits (EVANS, 1980).

(iii) the high proportion of P205 is strictly related to apatite occurrence which is likely to be of biogenic origin. This mineral is responsible for the high phosphorus content of the majority of the Phanerozoic ironstones.

(iv) The fluorine content, similar to that seen in crustal materials, (because of abundance of fluorapatite within igneous rock-forming minerals) is linked to the apatite. In some fish bones the fluorine content can reach 22,100 ppm (WEDEPOHL, 1974), whereas within sedimentary apatites it ranges from 2 to 5% (SLANSKY, 1980);

(v) MgO, Na_2O, and K_2O, are mobile elements, and are low in concentration in all types of ironstones. The relative high average value of CaO is only induced from the Ca-rich ironstones;

(vi) concentrations of Co, Ni, Cr, Pb and Zn are higher than crustal material. The Co range is similar to values of other ironstones. Co, Ni and Cr, usually very mobile elements, are abnormally high when compared to other Saharan ironstones (GUERRAK, unpublished data). Zinc, primarly occurring in the

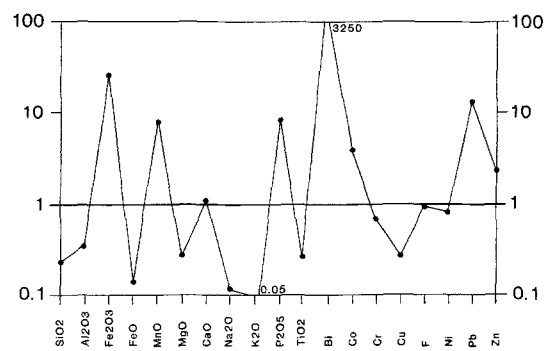

Fig. 11. Comparison of major and minor elements' average versus crustal abundance.

structure of silicates and oxides (WEDEPOHL, 1974) goes into solution during chemical weathering, but its low concentrations in surface waters, indicates a restricted mobility. However it is mainly absorbed by clay minerals such as ferruginous silicates (particularly chamosite) and iron oxides or hydroxides (hematite and goethite);

(vii) lead is weakly linked to iron, but mostly accumulated in clay minerals (WEDEPOHL, 1974) such as chamosite. High Pb values found within Banded Ironstones of Mauritania (BESNUS et al. 1969) were related to meteoric sources.

(viii) Copper concentrations was lower than that it is in crustal material: this was also reported by JAMES (1966).

The distribution of minor elements seems parallel to those found in shales, and particularly chloritic shales (JAMES, 1966). This may confirm the suggested importance of chamosite in the genesis of oolitic ironstone.

Conclusion

The discussion of iron transport and oolithic accretion mechanisms have been developed in other papers (GUERRAK & CHAUVEL, 1985; CHAUVEL & GUERRAK, 1986; GUERRAK, 1987). We have here discussed some aspects specific to the Ahnet s. l. area.

The data recorded in this study corroborate our previous reported observations and conclusions on Saharan ironstones. The ironstone was primarly developed in tranquil conditions by intrasedimentary processes within an iron-rich silicated mud (JAMES & VAN HOUTEN, 1979; VAN HOUTEN & PURUCKER, 1985; CHAUVEL & GUERRAK, 1986).

Probably in the same way, ferriferous coated grains are formed in Recent deposits such as Lake Chad (LEMOALLE & DUPONT, 1973), Ogooue delta in Gabon (GIRESSE, 1969), Orinoco and Niger deltas (PORRENGA, 1965) and Mahakam delta in Indonesia (ALLEN et al., 1979). After accretionary periods, detrital ooliths appeared in the sediments, before their final incorporation in the ironstone beds.

The oolitic ironstone sedimentation seems to be induced by several pulses, disturbing the major sedimentary cycles. Therefore the oolitic ironstone deposition can serve as a useful indicator of minor cycles (sub-cycles).

Ironstones formed in cratonic sedimentation environments, on the borders of large shallow epicontinental seas, disappeared when the depth increased.

The ironstone deposits are a branch of the widespread Oolitic Ironstone Belt (GUERRAK, 1987), which extends from the Rio de Oro (SOUGY, 1964) and Morocco (DESTOMBES, 1977), to Libya (NAKHLA et al., 1978; CHAUVEL & MASSA, 1981; VAN HOUTEN & KARAZEK, 1981). This belt, closely linked to the Gondwanan evolution, contains numerous Paleozoic ironstone occurrences which are Ordovician, Silurian and Devonian in age and are related to alternating cold and temperate climates. The problem of the distribution of oolitic ironstones and their paleolatitudinal location cannot easily be solved. Indeed, according to the more common continental drift reconstructions (MOREL & IRVING, 1978; SCOTESE et al., 1979; BAMBACH et al., 1980; SPJELDNAES, 1981; BOUCOT & GRAY, 1983; HARGRAVES & VAN HOUTEN, 1985), one would locate Saharan areas within assembled Gondwana, particularly during Devonian times. However, there is a lack of consensus for the location of the Devonian pole. The Msissi norite (Morocco) which was one of the paleomagnetic reference for Devonian pole in Africa (HAILWOOD, 1974; LIVERMORE et al., 1985) is in fact of Upper Jurassic age (136–139 Ma; SALMON et al., 1986). The location of North-Africa would be latitudes 30° and 60° south at this time and corresponds to the present day temperate zone. This relatively mild climate is not incompatible with the deposition of oolitic ironstone in this area. On the other hand, the source of iron would appear to be associated with a remote southeastern continent probably related to the Pan-African mobile Belt of Nigeria and the Congo Shield (Fig. 12). This is suggested by the paleocurrent directions (BEUF et al., 1971), connected with ice-flow (BIJU-DUVAL et al., 1981), the northwestward slope of the Basement and of the Cambro-Ordovician rocks, and the great maturity of the detrital material. In any case, the source of iron cannot be related to a hot and humid climate. Its origin some 2000–3000 km south (60–90° S latitude) of the present deposits would place the original sedimentary environments in a cold area. For explaining some oolitic ironstone occurrences, HECKEL & WITZKE (1979) and VAN HOUTEN & BHATTACHARYYA (1982) invoked a supplementary influence of warm currents flooding the Gondwana margin. The process of ironstone formation does not necessarily involve an intertropical warm climate as stated by WOPFNER & SCHWARZBACH (1976) with important biorhexistasy phenomena (ERHART, 1961) for iron concentration, but at most, stages of continental preconcentration. The iron content of the rivers (which are supposed to have been the main iron transport agent), as indicated by LIVINGSTONE (1963), BERNER (1970) or TAYLOR & MC LENNAN (1985), seems to be independant of the climate. DICKEY (1968) estimated 4.7 million tons per year the pre-

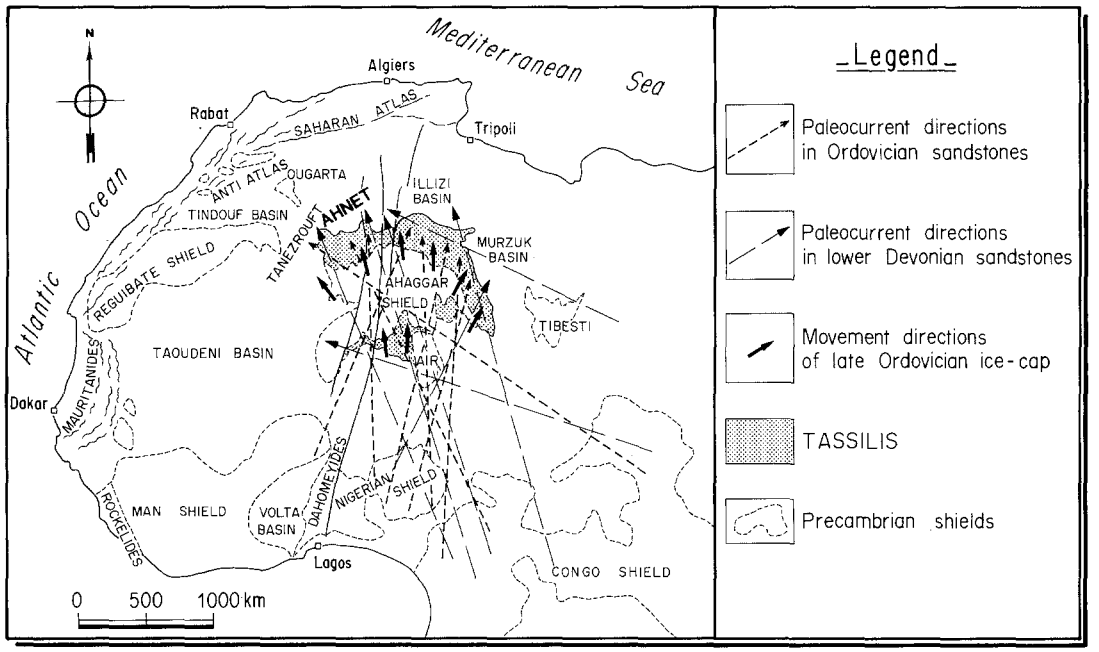

Fig. 12. Supposed iron flow directions and related source (data after BEUF et al., 1971).

cipitation of iron into the Aral sea (Soviet Central Asia); 97 % of iron carried by rivers being in the form of suspended matter and 3 % in solution. In other respects, transportation of iron (mostly in surface oxide films linked with suspended clays, CAROLL, 1958; JAMES, 1966) by meandering to anastamosing fluvial networks on a relatively flat continent, coincided with a period of general tectonic stability. The variations of detrital influx corresponding to the sedimentary cycles was accentuated by epeirogenic movements. The latter probably influenced the paleotopographies and thus influenced too the bulk solid discharge of the rivers.

Acknowledgements

The National Mining Research Company of Algeria (EREM) provided field support of the project and laboratory analyses. For this, the author gratefully acknowledges A. Slougui, T. Sahli and A. Belaid. I am greatly indebted to A. Moussine-Pouchkine (Geological and Geophysical Research Center, Montpellier, France) for his assistance in the field and for the stratigraphical data. J. J. Chauvel (University of Rennes) reviewed an early version of the manuscript and made helpful suggestions. Discussions with J. Fabre (National Center of Scientific Research, Grenoble, France) contributed to a better comprehension of the African geology. Reviewers of Geologische Rundschau are acknowledged for critical review and improving the English.

References

ALLEN, G. P., LAURIER, D. & THOUVENIN, J. (1979): Etude sédimentologique du delta de la Mahakam. – Notes Mém. Com Fr. Pétroles, **15**, 11–156.

ALLEN, J. R. L. (1974): Studies in fluviatile sedimentation: lateral variation in some fining-upwards cyclothems from the Red Marls, Pembrokeshire. – Geol. Journ. **9**, 1–16.

BAILEY, S. W. (1980): Structures of layers silicates. – In: Crystal structures of clay minerals and their X-ray identification. G. W. Brindley & G. Brown (ed.). Mineralogical society, London, **5**, 1–123.

BAYLISS, P. (1975): Nomenclature of the triotahedral chlorites. – Canadian Mineralogist, **13**, 178–180.

BENNACEF, A., BEUF, S., BIJU-DUVAL, B., DE CHARPAL, O., GARIEL, O. & ROGNON, P. (1971): Example of Cratonic Sedimentation: Lower Paleozoic of Algerian Sahara. – Am. Asso. Petro. Geol. Bull, **55**, 12: 2225–2245.

BERTRAND-SARFATI, J., FABRE, J. & MOUSSINE-POUCHKINE, A. (1977): Géodynamique des aires sédimentaires cratoniques: quelques exemples sahariens. – Bull. Cent. Rech. Explo. Prod. Elf-Aquitaine, **1**, 217–231.

BESNUS, Y., BRONNER, G., MOSSER, C. & OKSENGORN, S. (1969): Etudes géochimiques et minéralogiques sur la province ferrifère du Tiris (Précambrian de la Dorsale Reguibate, Fort-Gouraud, Mauritanie). – Bull. Serv. Carte géol. Als. Lorr., **22**, 4, 311–328.

Beuf, S., Biju-Duval, B., De Charpal, O., Rognon, P., Gariel, O. & Bennacef, A. (1971): Les grès du Paléozoïque inférieur du Sahara. Technip., Paris, 465p.

Biju-Duval, B., Deynoux, M., & Rognon, P. (1981): Late Ordovician tillites of the Central Sahara. – In: Hambrey, M. J., & Harland, W. B. (Ed.): Earth's Pre-Pleistocene Glacial Record, 99–107, Cambridge University Press (England).

–, De Charpal, O. & Merabet, O. (1966): Constance des directions de courant dans les grès de base du Cambro-Ordovicien sur le pourtour du Hoggar – Compt. Rend. Acad. Sci. Paris, **262**, 48–50.

Burollet, P. F. & Busson, G. (1983): Plate-formes et bassins. Danger d'un actualisme exagéré. – Notes Mém. Comp. Fr. Pétroles, **18**, 9–16.

Caroll, D. (1958): Role of clay minerals in the transportation of iron with special reference to the Clinton iron ore deposits. – Econ. Geol., **45**, 755–770.

Chauvel, J. J. & Guerrak, S. (1986): Oolitization of iron formations. Examples of North-African deposits. – 7th Regional Meeting of Sedimentology, Krakow, 45–46.

– & Massa, D. (1981): Paléozoïque de Libye occidentale. Constantes géologiques et pétrographiques. Signification des niveaux ferrugineux oolithiques. – Notes Mém. Com. Fr. Pétroles, **16**, 25–66.

Conrad, J. & Lemosquet, Y. (1984): Du craton vers sa marge: évolution sédimentaire et structurale du bassin Ahnet – Timimoun – Béchar (Sahara algérien) au cours du Carbonifère; données paléoclimatiques. – Bull. Soc. Géol. France, 7, XXVI, 6, 987–994.

Dapples, E. C. (1967): Diagenesis of sandstones. – In: Diagenesis in sediments. G. Larsan & G. V. Chilingar (ed.). Develop. sediment. Elsevier, Amsterdam, **8**, 91–125.

Destombes, J. (1977): Les gisements de minerai de fer du Maroc. – In: The Iron Ore deposits of Europe and adjacent Areas. A. Zitzmann (ed.). Subcommission for the Metallogenic Map of the World. – Hannover, 1: 29–236.

Dickey, P. A. (1968): Contemporary nonmarine sedimentation in Soviet Central Asia. – Am. Assoc. Petrol. Geol. Bull., **52**, 2396–2421.

Donzeau, M., Fabre, J. & Moussine-Pouchkine, A. (1981): Comportement de la dalle saharienne et orogenèse varisque. Essai d'interprétation. – Bull. Soc. Hist. Nat. Afrique du Nord, Alger, **69**, 3/4, 137–172.

Dubois, P., Beuf, S. & Biju-Duval, B. (1967): Lithostratigraphie du Dévonien inférieur gréseux du Tassili N'Ajjer. – Mém. Bur. Rech. Géol. Minières, Fr., **33**, 227–235.

Erhart, H. (1955): Biostasie et Rhexistasie. Esquisse d'une théorie sur le rôle de la pédogenèse en tant que phénomène géologique. – Compt. Rend. Acad. Sci. Paris, **241**, 1218–1220.

Evans, A. M. (1980): An Introduction to Ore Geology. Geosciences Texts. Volume **2**. Blackwell Scientific Publications, Oxford, 231p.

Fabre, J. (1976): Introduction à la géologie du Sahara algérien. – S. N. E. D. Alger, 422p.

– & Moussine-Pouchkine, A. (1971): Régressions et transgressions permo-carbonifères sur le nord-ouest de la plate-forme africaine: épirogenèse ou variation eustatique. – Bull. Soc. Géol. France, 7, XIII, 1/2, 140–145.

Follot, J. (1952): Ahnet et Mouydir. – 19th Int. Geol. Congress, Algiers, **1**, 1, 80p.

Giresse, P. (1969): Etude des différents grains ferrugineux authigènes des sédiments sous-marins au large du delta de l'Ogooué (Gabon). – Sciences de la Terre, Nancy, **1**, 27–62.

Gross, G. A. (1970): Nature and occurrence of iron ore deposits. – In: Survey of World Iron Ore Resources. New York. United Nations Publ, 13–31.

Guerrak, S. (1987): Paleozoic oolitic ironstones of the Algerian Sahara: a review. – Jour. Afri. Earth. Sc. **6**, 1, 1–8.

– & Chauvel, J. J. (1985): Les minéralisations ferrifères du Sahara algérien. Le gisement de fer oolithique de Mecheri Abdelaziz (bassin de Tindouf). – Mineral. Deposita, **20**, 249–259.

Hallam, A. & Bradshaw, M. J. (1979): Bituminous shales and oolitic ironstones as indicators of transgressions and regressions. – Tl. Geol. Soc. Lond., **136**, 157–164.

Han, T. M. (1986): Origin of magnetite in low-grade metamorphic Precambrian Iron Formation. – 7th Iagod Symp. Lulea. Abst. Terra Cognita. (3), 563.

Hargraves, R. B. & Van Houten, F. B. (1985): Paleogeography of Africa in Early-Middle Paleozoic. Paleomagnetic and stratigraphic constraints and tectonic implications. – 13th colloquium of African Geology, St Andrews. CIFEG. Occ. Pub. 3, 160–161.

Harms, J. C., Southard, J. B. & Walker, R. G. (1982): Structures and sequences in clastic rocks. – Soc. Eco. Pal. Mineralogists. Short course, **9**, 4.1–4.19.

Heckel, P. H. & Witzke, B. W. (1979): Devonian world palaeogeography determined from distribution of carbonate and related lithic palaeoclimatic indicators. – In: M. R. House, C. H. Scruton & M. G. Basset (Eds.), Spec. Pap. in Paleon., **23**, 99–123.

Hey, M. R. (1954): A new review of the chlorite. – Min. Magazine, XXX, 224, 277–292.

James, H. L. (1966): Chemistry of the Iron-rich Sedimentary Rocks. – U. S. Geol. Surv. Prof. Pap. 440W. 61p.

– & Van Houten, F. B. (1979): Miocene goethitic and chamositic oolites, north-eastern Columbia. – Sedimentology, **26**, 125–133.

Kilian, C. (1922): Aperçu général de la structure des Tassilis des Ajjers. – Compt. Rend. Acad. Sci. Paris, 175, **19**, 825–827.

Kimberley, M. M. (1978): Paleoenvironmental classification of iron formations. – Econ. Geol. **73**, 215–229.

– (1981): Oolitic Iron Formations. – In: Handbook of Stratabound and Stratiform Ore Deposits. K. H. Wolf, (Ed.), **9**, 25–76.

Krauskopf, K. B. (1957): Separation of manganese from iron in sedimentary processes. Geochim. Cosmochim. – Acta, **12**, 61–68.

Krumbein, W. C. & Dacey, M. F. (1969): Markov chains and Embedded Markov chains in Geology. – Math. Geol. **1**, 1: 79–96.

Legrand, P. (1985): Le Dévonien du Sahara algérien. – Proc. Int. Symp. Devonian System, Calgary, 245–284.

– (1985): Lower Palaeozoic rocks of Algeria. – In: Lower Palaeozoic of north-western and west central Africa. C. H. Holland (Ed.) Wiley, New-York: 5–89.

LEMOALLE, J. & DUPONT, B. (1973): Iron-bearing ooliths and the present conditions of Iron Sedimentation in Lake Chad (Africa). – In: Ores in Sediments, G. C. Amstutz & A. J. Bernard (Eds). Springer-Verlag, New-York, 167–178.

LIVINGSTONE, D. A. (1963): Chemical composition of Rivers and Lakes. – U. S. Geol. Surv. Prof. Paper, 440 G, 63 p.

MASSON, B. (1958): Principles of Geochemistry. – Wiley, New-York, 310 p.

MENCHIKOFF, N. (1957): Les grandes lignes de la géologie saharienne. – Rev. Geog. Phy. Geo. Dyn. Paris, 1, 1, 37–45.

MOREL, P. & IRVING, E. (1978): Tentative Paleocontinental maps for the early Phanerozoic and Proterozoic. – Jour. Geol., **86**, 5, 535–562.

MOUSSINE-POUCHKINE, A. (1962): Les constructions recifales du Dévonien moyen du pays-bas de l'Ahnet (Sahara central, Algérie). – Soc. Hist. Nat. Afri. Nord, Alger, **62**, (3–4), 79–88.

– (1976): La sédimentation marine du Dévonien moyen et supérieur sur la plate-forme saharienne (Sahara occidental et central, Algérie). Courrier du C. N. R. S., Paris, **3**, 102–103.

NAKHLA, F. M., SMYKATZ-KLOSS, W. & EL MANEI, M. I. (1978): Magnetite Ooids from Wadi Al-Shati Iron Ores, Fezzan, Libya, Chemie der Erde, **37**, 206–220.

ODIN, G. S. & GALE, N. H. (1982): Géochimie et géochronologie isotopiques. Mise à jour de l'échelle des temps calédoniens et hercyniens. – Compt. Rend. Acad. Sci. Paris, **294**, 2, 453–457.

ORCEL, J. (1927): Recherce sur la composition chimique des chlorites. – Bull. Soc. Miner., **50**, 75–456.

PORRENGA, D. H. (1965): Chamosite in recent sediments of the Niger and Orinoco deltas. – Geol. En Mijnb., **44**, 400–403.

ROUTHIER, P. (1963): Les gisements métallifères. – Géologie et principes de recherches. Masson, Paris, 1284 p.

SELLEY, R. C. (1970): Studies of sequence in sediments using a simple mathematical device. – Q. Jour. Geol. Soc. London, **45**, 557–581.

SCOTESE, C. R., BAMBACH, R. K., BARTOW, C., VAN DER VOO, R. & ZIEGLER, A. M. (1979): Paleozoic base maps. Jour. Geol., **87**, 3, 217–277.

SLANSKY, M. (1980): Géologie des phosphates sédimentaires. – Bureau Rech. Geol. et Minières. Mém. 114, 92 p.

SOUGY, J. (1964): Les formations paléozoïques du Zemmour Noir (Mauritanie septentrionale). – Ann. Fac. Sc. Dakar, **15**, 695 p.

SPJELDNAES, N. (1981): Lower Palaeozoic Palaeoclimatology. – In: Lower Palaeozoic of the Middle East, Eastern and Southern Africa, and Antarctica. C. H. Holland (Ed.). Wiley, New-York, 199–256.

TAYLOR, S. R. & MC LENNAN, S. M. (1985): The Continental Crust: its Composition and Evolution. – Blackwell Scientific Pub. Oxford. 312 p.

TEYSSEN, T. A. L. (1984): Sedimentology of the Minette oolitic ironstones of Luxembourg and Lorraine: a Jurassic subtidal sandwave complex. – Sedimentology, **31**, 195–211.

VAN HOUTEN, F. B. & KARASEK, R. M. (1981): Sedimentologic framework of late Devonian iron formation, Shatti Valley, West Central Libya. Jour. Sedim. Petrology, **51**, 415–427.

– & BHATTACHARYYA, D. P. (1982): Phanerozoic oolitic ironstones. – Geologic Record and Facies Model. Annual Review of Earth and Planetary Sciences., **10**, 441–457.

– & PURUCKER, M. E. (1984): Glauconitic Peloids and Chamositic Ooids. Favorable Factors, Constraints, and Problems. – Earth. Sci. Rev., **20**, 211–243.

– & PURUCKER, M. F. (1985): On the origin of glauconitic and chamositic granules. Geo-Marine Letters, **5**, 47–49.

WEDEPOHL, K. H. (1974): Handbook of Geochemistry. Springer-Verlag, Berlin. 5 volumes.

WOPFNER, H. & SCHWARZBACH, M. (1976): Ore deposits in the light of Palaeoclimatology. – In: Handbook of Stratabound and stratiform ore deposites. K. H. Wolf (Ed.). Elsevier, Amsterdam, **3**, 43–92.